Mon. Not. R. Astron. Soc. **000**, 1–5 (2009) Printed 8 January 2010 (MN LATEX style file v2.2)

High resolution AMI Large Array imaging of spinning dust sources: spatially correlated 8 μm emission and evidence of a stellar wind in L675*

AMI Consortium: Anna M. M. Scaife[1,2]†, David A. Green[1], Guy G. Pooley[1], Matthew L. Davies[1], Thomas M. O. Franzen[1], Keith J. B. Grainge[1,3], Michael P. Hobson[1], Natasha Hurley-Walker[1], Anthony N. Lasenby[1,3], Malak Olamaie[1], John S. Richer[1,3], Carmen Rodríguez-Gonzálvez[1], Richard D. E. Saunders[1,3], Paul F. Scott[1], Timothy W. Shimwell[1], David J. Titterington[1], Elizabeth M. Waldram[1] & Jonathan T. L. Zwart[4]

[1] *Astrophysics Group, Cavendish Laboratory, J J Thomson Avenue, Cambridge CB3 0HE*
[2] *Dublin Institute for Advanced Studies, 31 Fitzwilliam Place, Dublin 2, Ireland*
[3] *Kavli Institute for Cosmology Cambridge, Madingley Road, Cambridge, CB3 0HA*
[4] *Columbia Astrophysics Laboratory, Columbia University, 550 West 120th Street, New York 10027, USA*

Accepted —; received —; in original form 8 January 2010

arXiv:0910.4011v2 [astro-ph.GA] 8 Jan 2010

ABSTRACT

We present 25″ resolution radio images of five Lynds Dark Nebulae (L675, L944, L1103, L1111 and L1246) at 16 GHz made with the Arcminute Microkelvin Imager (AMI) Large Array. These objects were previously observed with the AMI Small Array to have an excess of emission at microwave frequencies relative to lower frequency radio data. In L675 we find a flat spectrum compact radio counterpart to the 850 μm emission seen with SCUBA and suggest that it is cm-wave emission from a previously unknown deeply embedded young protostar. In the case of L1246 the cm-wave emission is spatially correlated with 8 μm emission seen with *Spitzer*. Since the MIR emission is present only in *Spitzer* band 4 we suggest that it arises from a population of PAH molecules, which also give rise to the cm-wave emission through spinning dust emission.

Key words: Radiation mechanisms: general – ISM: general – ISM: clouds – stars: formation

1 INTRODUCTION

The complete characterization of microwave emission from spinning dust grains is a key question in both astrophysics and cosmology. It probes a region of the electromagnetic spectrum where a number of different astrophysical disciplines overlap. It is important for CMB observations in order to correctly characterise the contaminating foreground emission; for star and planetary formation it is important because it potentially probes a regime of grain sizes that is not otherwise easily observable.

Although a number of objects have now been found to exhibit anomalous microwave emission, attributed to spinning dust, it is still unclear what differentiates those objects from the many other seemingly similar targets that do not show the excess. In the specific case of dark clouds the recent AMI sample (AMI Consortium: Scaife et al. 2009; hereinafter Paper I) of fourteen Lynds Dark Nebulae found an excess in only five.

It has been suggested that cm-wave emission from spinning dust is emitted by a population of ultra-small grains (Draine & Lazarian 1998). These ultra-small grains are thought to exist mainly in the form of single polycyclic aromatic hydrocarbon (PAH) molecules. PAH molecules are generally detected through their narrow line emission features in the MIR. For these emission features to be observed the PAH molecules must be exposed to a strong source of UV flux. Since this flux is generally absent in the case of dark clouds, the microwave emission from the rotation of PAH molecules may be the only way to study the very small grain population in these objects.

It is also known that radio continuum emission in dark clouds may arise from ionized gas associated with a stellar outflow. When a luminous star is present this arises either as the result of a compact HII region or an ionized stellar wind. In the case of very young

* We request that any reference to this paper cites "AMI Consortium: Scaife et al. 2010"

† E-mail: ascaife@cp.dias.ie

low luminosity stars radio continuum emission may be also be detected. In this instance it is generally attributed to the presence of a partially ionized ($0.02 \leqslant x_e \leqslant 0.35$; Bacciotti & Eislöffel 1999) stellar wind (Wright & Barlow 1975; Panagia & Felli 1975), or possibly a neutral wind which has been shock-ionized further from the central source by impacting on a dense obstacle (Curiel et al. 1989).

In this paper we present follow-up observations of the five AMI Small Array (SA) spinning dust detections (Paper I) at higher resolution with the AMI Large Array (LA) over the same frequency range. All co-ordinates in this paper are J2000.0.

2 OBSERVATIONS

AMI comprises two synthesis arrays, one of ten 3.7 m antennas (SA) and one of eight 13 m antennas (LA), both sited at Lord's Bridge, Cambridge (AMI Consortium: Zwart et al. 2008). The telescope observes in the band 13.5–17.9 GHz from which eight 0.75 GHz bandwidth channels are synthesized. In practice, the two lowest frequency channels (1 & 2) are not generally used due to a lower response in this frequency range and interference from geostationary satellites.

Observations of five Lynds dark nebulae selected from the original AMI SA sample were made in 2009 February–March using the AMI LA. The co-ordinates of these fields are listed in Table 1 along with the size of the AMI LA synthesized beam towards each object and the r.m.s. noise measured outside the primary beam on the CLEANed maps. We note that the AMI LA observation of L1246 is towards the north–east of this cloud where anomalous emission was detected by the AMI SA and does not cover the same area as the original SCUBA observation.

Data reduction was performed using the local software tool REDUCE, see Paper I for more details. Flux calibration was performed using short observations of 3C286 near the beginning and end of each run. We assumed I+Q flux densities for this source in the AMI LA channels consistent with the frequency dependent model of Baars et al. (1977), $\simeq 3.3$ Jy at 16 GHz. As Baars et al. measure I and AMI LA measures I+Q, these flux densities include corrections for the polarisation of the calibrator source derived by interpolating from VLA measurements. A correction is also made for the changing intervening air mass over the observation. The phase was calibrated using interleaved observations of calibrators selected from the Jodrell Bank VLA Survey (JVAS; Patnaik et al. 1992). After calibration, the phase is generally stable to 5° for channels 4–7, and 10° for channels 3 and 8. The FWHM of the primary beam of the AMI LA is $\approx 6'$ at 16 GHz.

Reduced data were imaged using the AIPS data package. CLEAN deconvolution was performed using the task IMAGR which applies a differential primary beam correction to the individual frequency channels to produce the combined frequency image. Deconvolved maps were made from both the combined channel set, see Fig. 1, and for individual channels. The broad spectral coverage of AMI allows a representation of the spectrum between 14.3 and 17.9 GHz to be made independently of other telescopes and in what follows we use the convention: $S \propto \nu^{-\alpha}$, where S is flux density, ν is frequency and α is the spectral index. All errors are quoted to $1\,\sigma$.

Table 1. AMI LA Lynds Dark Nebulae. Column [1] Name of cloud, [2] Right Ascension, [3] Declination, [4] AMI LA synthesized beam FWHM major axis, [5] AMI LA synthesized beam FWHN minor axis, and [6] r.m.s. noise fluctuations on the combined channel map.

Name	RA (J2000)	Dec (J2000)	$\Delta\theta_{\rm maj}$ (arcsec)	$\Delta\theta_{\rm min}$ (arcsec)	$\sigma_{\rm rms}$ ($\frac{\mu\rm Jy}{\rm bm}$)
L675	19 23 52.6	11 07 39	49.9	27.4	35
L944	21 17 40.8	43 18 08	36.5	31.2	31
L1103	21 42 10.2	56 43 44	32.0	26.3	25
L1111	21 40 27.1	57 48 10	39.4	30.8	29
L1246	23 25 30.1	63 38 30	31.2	26.9	25

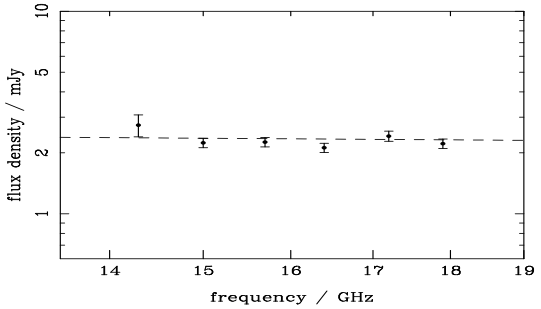

Figure 2. L675 Source A: data points are flux densities from AMI LA channels 3–8. The best-fit spectral index of $\alpha = 0.10 \pm 0.36$ is shown as a dashed line.

3 RESULTS

L675: The AMI LA observations of L675 show two obvious regions of compact emission, see Fig. 1. The first of these, slightly offset from the pointing centre, is coincident with both the peak of the AMI SA emission and also the compact emission seen at 850 μm by the SCUBA instrument (Visser et al. 2001; 2002). We denote this source "A" ($19^{\rm h}23^{\rm m}50\overset{\rm s}{.}5$, $+11^\circ07'44''$). The second, just outside the LA primary beam FWHM to the north-east, is coincident with the probable extragalactic point source identified as "B" ($19^{\rm h}24^{\rm m}02\overset{\rm s}{.}4$, $+11^\circ10'54''$) in the original AMI SA observations (Paper I).

Source A is completely unresolved by the AMI LA and shows a flat spectrum across the AMI band, $\alpha_{14.3}^{17.9} = 0.10 \pm 0.36$, consistent with free–free emission, see Fig. 2. This spectral index differs considerably from that measured by AMI SA. This is because the LA is not sensitive to the large scale emission seen with the SA. Indeed it seems likely that the emission seen by the two arrays arises from completely different sources.

L944: The original AMI SA observations of L944 revealed a compact region of emission to the north of the cloud, coincident with one side of the protostellar outflow. AMI LA observations, see Fig. 1, reveal this emission arises not from a point-like object but rather from a diffuse region of emission, the peak of which occurs at $21^{\rm h}17^{\rm m}42\overset{\rm s}{.}6$, $+43^\circ20'08''$. We estimate the flux spectrum by integrating the flux density from the primary beam corrected channel maps within a two arcminute radius of the LA pointing centre. This shows a steeply rising spectrum with $\alpha_{14.3}^{17.9} = -2.1 \pm 0.5$. This is consistent with that found from the AMI SA data, however this correspondence is not meaningful as the low signal to noise in the SA data precludes a precise estimate. The flux density found towards this region in the LA map is only marginally lower than that found from the comparatively coarser resolution SA map. This implies

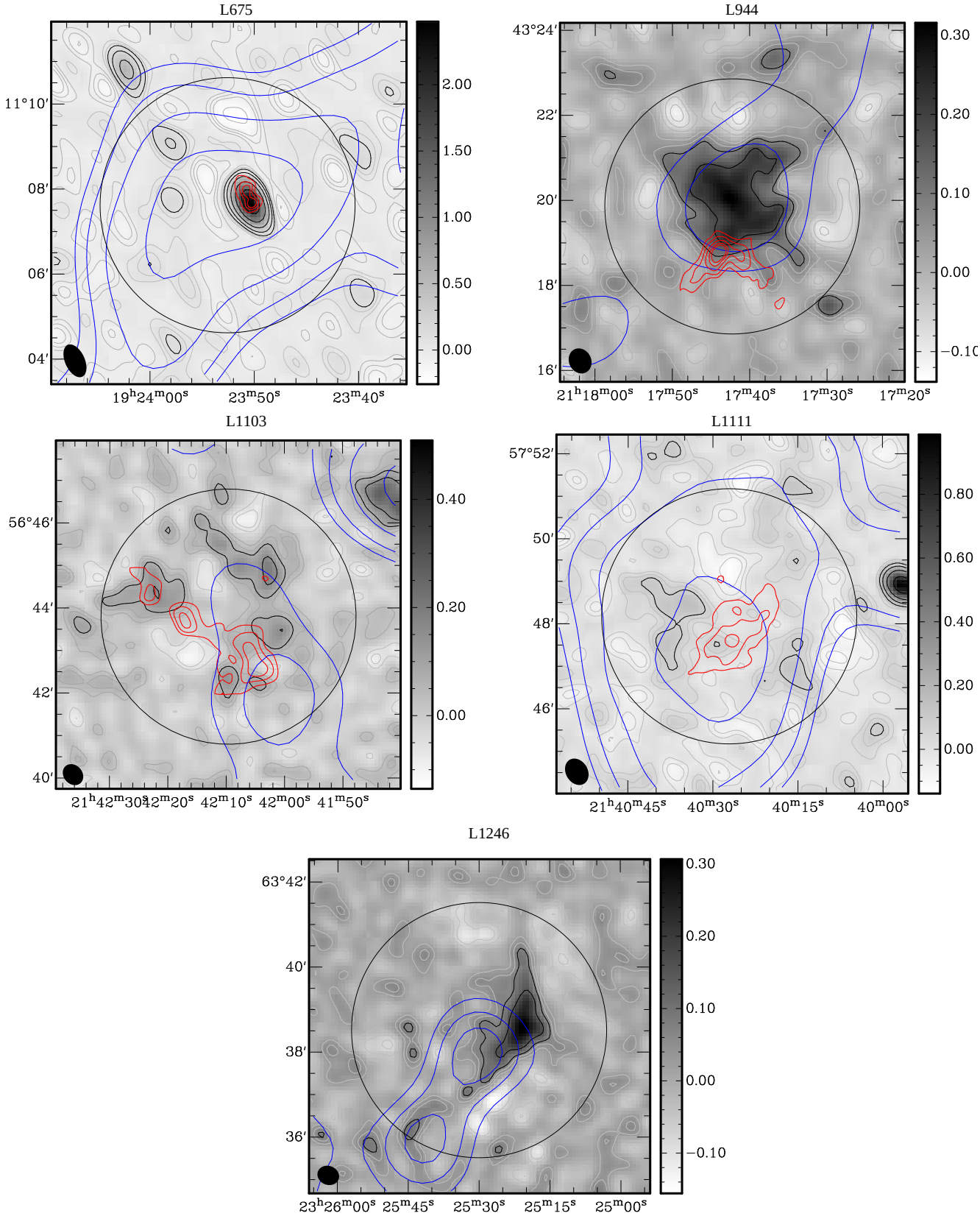

Figure 1. AMI LA combined channel data is shown as greyscale in units of mJy/beam, grey conrtours at $-6, -3, \pm 2, \pm 1\sigma$ and black contours at 3, 6, 12, 24 σ etc. SCUBA 850 μm data is shown as red contours with levels as in Visser et al. (2001; 2002) for the all clouds except L1246. The AMI LA observation of L1246 does not cover the region observed by SCUBA. AMI SA data is shown as blue contours with levels as in Paper I. The AMI LA primary beam FWHM is shown as a circle and the synthesized beam as a filled ellipse in the bottom left corner.

Table 2. Integrated flux densities in mJy for AMI LA observations of L675, L944 and L1246. Errors are calculated as $\sigma = \sqrt{(0.05S)^2 + \sigma_{\rm rms}^2}$, where $\sigma_{\rm rms}$ is the r.m.s. noise in the individual channel map.

	Freq. (GHz)												
Name	14.3		15.0		15.7		16.4		17.2		17.9		α
L675	2.74	±0.34	2.24	±0.12	2.26	±0.12	2.12	±0.11	2.42	±0.14	2.22	±0.12	+0.10±0.36
L944	-		2.03	±0.11	2.40	±0.13	2.89	±0.15	2.86	±0.15	-		−2.11 ± 0.49
L1246	-		0.62	±0.18	0.55	±0.03	0.62	±0.03	0.58	±0.04	-		−0.40 ± 0.82

that the emission comes not from one smooth extended region that is partially resolved out by the LA baselines, but from a collection of smaller fragments or filaments. These fragments are unresolved by either array, although the granularity becomes more evident in the higher frequency channels of the LA. The amount of flux lost in channels 5 to 8 relative to channel 4 is significantly smaller than would be expected from a Gaussian source of similar dimensions.

L1103 and L1111: AMI LA observations of L1103 and L1111 do not show any distinct regions of compact cm-wave emission. The diffuse patches of low level emission present within the primary beam towards both sources are indicative of larger scale structures which have been resolved out by the synthesized beam. We can provide an estimate of the flux density seen towards these objects with the LA by fitting and removing a tilted plane baselevel at the primary beam FWHM. From the combined channel data this gives $S_{16} = 5.1 \pm 0.6$ mJy and $S_{16} = 2.4 \pm 0.3$ mJy for L1103 and L1111, respectively. These values indicate that the flux loss is considerable: approximately 45% and 96%. The sensitivity of these LA observations is much greater than those of the SA and it is possible that the patchy emission in these fields corresponds to enhancements in the extended emission which are below the detection threshold in the SA data.

L1246: AMI SA observations towards L1246 did not show any excess emission coincident with the SCUBA identification of the dark cloud, but did reveal a region of emission $\approx 2'$ to the north–east of the cloud, in a region not covered by the SCUBA map, which had no counterpart in the lower frequency observations. AMI LA observations of this NE region show an arc of emission (peak: $23^{\rm h}25^{\rm m}20\overset{\rm s}{.}4$, $+63^\circ38'40''$), see Fig. 1. We assess the spectral behaviour of this object in two ways. Firstly, we estimate the flux density of the arc itself. We fit and remove a tilted plane baselevel within an irregular polygon drawn around the object and integrate the remaining flux. Secondly, we fit a tilted plane baselevel to a circle at the primary beam FWHM and integrate all the flux above this baselevel within that radius. Both methods give consistent results, as might be expected since the primary beam is relatively empty otherwise. From the first method we find a spectral index $\alpha_{15.0}^{17.9} = -0.40 \pm 0.87$, and from the second $\alpha_{15.0}^{17.9} = -0.47 \pm 0.82$.

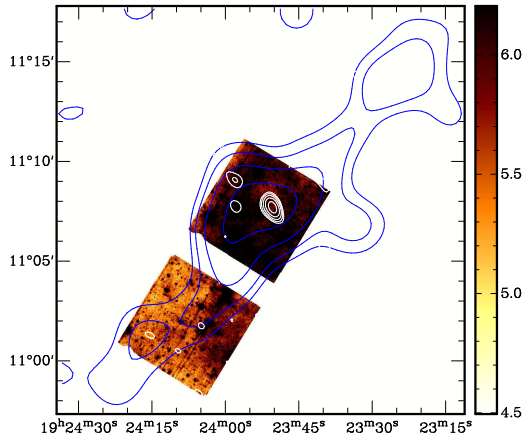

Figure 3. L675: AMI LA combined channel data is shown as white contours at 3, 6, 12 σ etc. *Spitzer* Band 4 data is shown as greyscale in MJy/sr, and is saturated at both ends to emphasise the structure present. AMI SA data is shown as blue contours as in Fig. 1.

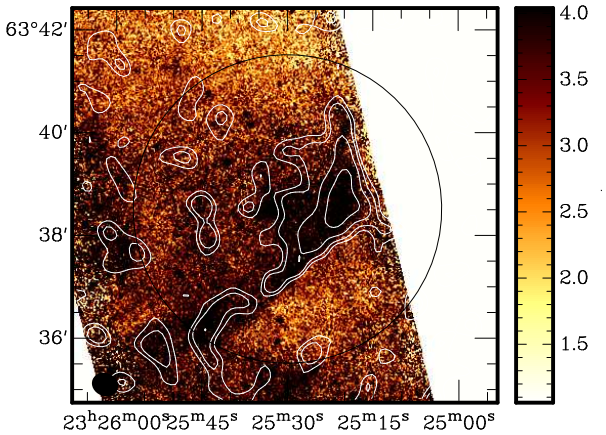

Figure 4. L1246: AMI LA combined channel data is shown as white contours at 1, 2, 4, 8 σ etc. *Spitzer* Band 4 data is shown as greyscale in MJy/sr, saturated at both ends of the scale to emphasise the structure present. The AMI LA primary beam is shown as a circle and the synthesized beam as a filled ellipse in the bottom left corner.

4 DISCUSSION AND CONCLUSIONS

L675 and L1246 have archival *Spitzer* IRAC data, which shows in both cases a significant amount of emission in Band 4 (6.4–9.4 μm) and very little in the other three (3.2–3.9, 4.0–5.0 and 4.9–6.4 μm, respectively). In the case of L675 this emission is present on a very large scale, see Fig. 3. The emission seen at 16 GHz with the AMI SA appears on a similar scale, however the small field of view of the *Spitzer* data precludes a more detailed comparison. L1246 shows an arc of emission at 16 GHz which is also evident in *Spitzer* IRAC Band 4, see Fig. 4. This emission is again not present in Bands 1–3. In Band 4 it is present as an arc, coincident with that seen at 16 GHz in the AMI LA data.

Spitzer Band 4 contains two of the PAH emission lines, including the strongest (7.7 μm). Of the three other *Spitzer* bands only Band 1 contains an emission line (3.3 μm) and for ionized PAHs this line is expected to be significantly weaker. It is probable therefore that the MIR correlated cm-wave data seen in the AMI maps is a consequence of spinning dust emission from a popula-

tion of ionized PAH molecules. Neutral PAH molecules do not in general possess a permanent dipole moment and are therefore not expected to have rotational emission (Tielens 2008). This emission, the mechanism of which is described in detail by Draine & Lazarian (1998), arises from the intrinsic dipole moments of small dust grains, most likely to be PAH molecules, which emit power when they rotate. This rotation has a variety of contributing factors, the relative importance of which varies with grain environment. However, in the majority of cases excitation through collision with ions is predominant.

In the case of L675A, we must consider the possibility that we are observing a coincidental extragalactic radio source. Using the extended 9C survey 15 GHz source counts (Waldram et al. 2009), where $n(S) = 51(S/\mathrm{Jy})^{-2.15}\,\mathrm{Jy}^{-1}\,\mathrm{sr}^{-1}$, the probability that a source with flux density greater than 2 mJy lies within the FWHM of the AMI LA primary beam is 0.12, and only 0.01 within the SCUBA field. It is likely therefore that the radio source L675A is associated with the SCUBA core.

A further question is whether the cm-wave emission might be explained by thermal (Planckian) dust emission. A single greybody spectrum with a dust temperature, $T_\mathrm{d} \approx 27$ K, might be used to explain the LA flux density, however it would require a β of 0.6. Such a value would be unusual even for objects known to possess flattened dust tails, such as protoplanetary disks. This simple fit also neglects the flux lost by the AMI LA baseline distribution. SA observations have already shown this source to possess a significant amount of extended emission which would make this scenario even more unlikely.

The presence of a neutral or partially ionized wind from an outflow source that has been shocked through encountering a dense obstacle (Torrelles et al. 1985; Rodríguez et al. 1986) is used to understand the spectral indices seen towards exciting sources in the radio regime (Curiel et al. 1990; Cabrit & Bertout 1992). This model allows a spectral index range of 0.1 (optically thin) to -2 (optically thick), which explains results which deviate from the value of $\alpha = -0.6$ required by a spherically symmetric ionized wind (Wright & Barlow 1975; Panagia & Felli 1975). Using this model as described in Curiel et al. (1989; 1990) the radio emission is expected to be optically thin ($\tau = 0.1$), consistent with the spectral index seen across the AMI band. Assuming a distance of 300 pc and a stellar wind with a wind speed of 200 km s^{-1}, we can calculate that the AMI flux densities towards L675A are consistent with a mass loss of $3.5 \times 10^{-7}\,\mathrm{M}_\odot\,\mathrm{yr}^{-1}$. A mass loss such as this implies a mechanical luminosity from the wind of $L_\mathrm{mech} \approx 1.1\,\mathrm{L}_\odot$, comparable to the values found by Curiel et al for L1448.

The nature of the emission seen towards L944 with the AMI LA is uncertain. The spectral index of this emission is consistent with spinning dust emission or alternatively the optically thick component of free–free spectrum. Such a free–free spectrum might be exhibited at 16 GHz by ultra-compact HII regions. However a turn-over frequency above 16 GHz would have an extremely high mass and should therefore be obvious in sub-mm observations. This needs to be confirmed by either higher radio frequency measurements in order to measure the optically thin region of the spectrum and the turn-over, or sub-mm measurements to place constraints on the mass of such a region.

In conclusion, we have used the AMI LA to observe a sample of five Lynds Dark Nebulae selected as candidates for spinning dust emission from the AMI SA sample of Lynds Dark Nebulae (Paper I). Towards two of these clouds (L1103 and L1111) we detect only patchy diffuse emission characteristic of the presence of a larger structure which has been mostly resolved out.

Towards L675 we have observed flat spectrum compact cm-wave emission coincident with the SCUBA 850 μm emission from the same region. These characteristics suggest that this source is associated with a stellar wind from a deeply embedded young protostar.

We detect extended cm-wave emission to the North of the L944 SMM-1 protostar which displays spectral behaviour consistent with either spinning dust, or alternatively a collection of ultra-compact HII regions.

L1246 shows an arc of cm-wave emission which is coincident with emission seen in *Spitzer* Band 4. We suggest that this is an example of emission from a population of PAH molecules, seen in emission lines in the *Spitzer* data, and emission as a consequence of rapid rotation of the molecules in the cm-wave data.

5 ACKNOWLEDGEMENTS

We thank the staff of the Lord's Bridge Observatory for their invaluable assistance in the commissioning and operation of AMI. AMI is supported by Cambridge University and the STFC. NH-W, CR-G, TWS, TMOF, MO and MLD acknowledge the support of PPARC/STFC studentships. This work is based in part on archival data obtained with the Spitzer Space Telescope, which is operated by the Jet Propulsion Laboratory, California Institute of Technology under a contract with NASA. Support for this work was provided by an award issued by JPL/Caltech.

REFERENCES

AMI Consortium: Hurley-Walker N., et al., 2009, MNRAS, 396, 365
AMI Consortium: Scaife A. M. M., et al., 2009, arXiv:0908.1655
AMI Consortium: Scaife A. M. M., et al., 2008, MNRAS, 385, 809
AMI Consortium: Zwart J. T. L., et al., 2008, MNRAS, 391, 1545
Baars J. W. M., Genzel R., Pauliny-Toth I. I. K., Witzel A., 1977, A&A, 61, 99
Bacciotti F., Eislöffel J., 1999, A&A, 342, 717
Cabrit S., Bertout C., 1992, A&A, 261, 274
Clemens D. P., Yun J. L., Heyer M. H., 1991, ApJS, 75, 877
Curiel S., Raymond J. C., Moran J. M., Rodriguez L. F., Canto J., 1990, ApJ, 365, L85
Curiel S., Rodriguez L. F., Bohigas J., Roth M., Canto J., Torrelles J. M., 1989, ApL&C, 27, 299
Draine B. T., Lazarian A., 1998, ApJ, 508, 157
Lada C. J., 1985, ARA&A, 23, 267
Panagia N., Felli M., 1975, A&A, 39, 1
Patnaik A. R., Browne I. W. A., Wilkinson P. N., Wrobel J. M., 1992, MNRAS, 254, 655
Torrelles J. M., Ho P. T. P., Rodriguez L. F., Canto J., 1985, ApJ, 288, 595
Rodriguez L. F., Canto J., Torrelles J. M., Ho P. T. P., 1986, ApJ, 301, L25
Visser A. E., Richer J. S., Chandler C. J., 2001, MNRAS, 323, 257
Visser A. E., Richer J. S., Chandler C. J., 2002, AJ, 124, 2756
Waldram E. M., Pooley G. G., Davies M. L., Grainge K. J. B., Scott P. F., 2009, arXiv:0908.0066
Wright A. E., Barlow M. J., 1975, MNRAS, 170, 41

This paper has been typeset from a TEX/ LATEX file prepared by the author.